

Laminin assembles into separate basement membrane and fibrillar matrices in Schwann cells

Maria V. Tsiper and Peter D. Yurchenco*

Department of Pathology & Laboratory Medicine, Robert Wood Johnson Medical School, Piscataway, NJ 08854, USA

*Author for correspondence (e-mail: yurchenc@umdnj.edu)

Accepted 28 November 2001

Journal of Cell Science 115, 1005-1015 (2002) © The Company of Biologists Ltd

Summary

Laminins are important for Schwann cell basement membrane assembly and axonal function. In this study, we found that exogenous laminin-1, like neuromuscular laminins-2/4, formed two distinct extracellular matrices on Schwann cell surfaces, each facilitated by laminin polymerization. Assembly of one, a densely-distributed reticular matrix, was accompanied by a redistribution of cell-surface dystroglycan and cytoskeletal utrophin into matrix-receptor-cytoskeletal complexes. The other, a fibrillar matrix, accumulated in separate zones associated with pre-existing β 1-integrin arrays. The laminin-1 fragment E3 (LG-modules 4-5), which binds dystroglycan and heparin, inhibited reticular-matrix formation. By contrast, β 1-integrin blocking antibody (Ha2/5) prevented fibrillar assembly. Ultrastructural analysis revealed that laminin treatment induced the formation of a linear electron-dense extracellular matrix (*lamina densa*) separated from plasma membrane by a narrow lucent zone

(*lamina lucida*). This structure was considerably reduced with non-polymerizing laminin, fully blocked by E3, and unaffected by Ha2/5. Although it formed in the absence of type IV collagen, it was nonetheless able to incorporate this collagen. Finally, cell competency to bind laminin and form a basement membrane was passage-dependent. We postulate that laminin induces the assembly of a basement membrane on competent cell surfaces probably mediated by anchorage through LG 4-5. Upon binding, laminin interacts with dystroglycan, mobilizes utrophin, and assembles a 'nascent' basement membrane, independent of integrin, that is completed by incorporation of type IV collagen. However, the fibrillar β 1-integrin dependent matrix is unlikely to be precursor to basement membrane.

Key words: Schwann cell, Laminin, Collagen, Integrin, Dystroglycan, Utrophin

Introduction

Basement membranes are present along the outer (abaxonal) aspect of the Schwann cell sheath of peripheral nerves and contain α 2-, α 4-, and α 5-laminins (Chernousov and Carey, 2000; Patton et al., 1997). The importance of α 2-laminins for the neuromuscular axis is illustrated by the merosin-deficient (α 2-laminin-deficient) congenital muscular dystrophies that are accompanied by peripheral nerve defects (Matsumura et al., 1997; Shorer et al., 1995). Studies on mouse models of the disease have revealed that the peripheral nerve and muscular components are separate, with the former responsible for the spastic gait seen in affected animals (Kuang et al., 1998). Of note, a mutation found in the *dy^{2J}* mouse causes an in-frame deletion within α 2-domain VI (Sunada et al., 1995; Xu et al., 1994). α 2-Laminin extracted from the muscle of affected mice has considerably reduced polymerization activity (Colognato and Yurchenco, 1999). In several human dystrophies, mutations have been identified within both the α 2-short arm and the long arm G-domain (Guicheney et al., 1997). The short arm mediates polymerization while the globular (G) domain has five component modules that mediate β 1- and β 4-integrin interactions, dystroglycan binding, and heparin binding (reviewed by Colognato and Yurchenco, 2000).

A model of the assembly of basement membranes on cognate cell surface membranes is that laminin and type IV collagen receptors provide surface anchorage, concentrating

them and facilitating their self-assembly into ECM heteropolymers (Colognato et al., 1999; Colognato and Yurchenco, 2000). A number of investigators have proposed that both β 1-integrin and dystroglycan play critical roles in the mediation of assembly in various tissues (Brakebusch et al., 2000; DiPersio et al., 1997; Henry and Campbell, 1998; Lohikangas et al., 2001). However, it is unclear if these particular receptors constitute the cell surface anchors that mediate assembly (Cote et al., 1999; Sasaki et al., 1998). α -Dystroglycan is a mucinous glycoprotein that is noncovalently bound to transmembrane β -dystroglycan and present on Schwann cells. It is thought to link the LG modules of α 1- and α 2-laminins to the cytoskeleton through its interaction with cytoskeletal dystrophin and/or utrophin (reviewed by Henry and Campbell, 1996). Schwann cell integrins capable of interacting with laminins are α 1 β 1, α 6 β 1 and α 6 β 4, the first binding through α 1-domain VI and the latter two binding through G-domain (Colognato et al., 1997; Colognato and Yurchenco, 2000; Einheber et al., 1993; Yurchenco et al., 1997). The Schwann cell expression pattern of these receptors changes during development and in response to specific physiological processes (Fernandez-Valle et al., 1994; Jaakkola et al., 1993; Stewart et al., 1997). Although their signaling mechanisms have been intensively studied, integrin roles in basement membrane formation are not well understood.

In this study we have investigated the contributions of

dystroglycan, β 1-integrin, and corresponding interacting long arm globular LG modules of laminin to Schwann cell basement membrane formation *in vitro*. Untreated Schwann cells, regardless of age, were found to express little, if any, endogenous α 1- or α 2-laminins on their surfaces. Later passaged Schwann cells became competent for basement membrane assembly, a process initiated by exogenous laminin. We found that dystroglycan and utrophin underwent a dynamic rearrangement with exogenous laminin into a dense (reticular) structure with classical ultrastructural features of a basement membrane. Formation of this architecture depended upon the participation of the terminal two laminin LG modules and polymerization. Moreover, collagen type IV was absent from the structures and was able to co-assemble into basement membrane-type structures in laminin-dependent manner when added exogenously. By contrast, β 1-integrin did not appear to be required for basement membrane assembly and instead mediated the formation of a separately defined fibrillar extracellular matrix (ECM). Finally, comparison of competent with incompetent cells implicates a third receptor or surface-anchoring molecule required for basement membrane assembly on Schwann cell surfaces.

Materials and Methods

Tissue culture

Schwann cells isolated from sciatic nerves from newborn Sprague Dawley rats were the kind gift of James Salzer (New York University). These cells were expanded *in vitro* for 5-10 passages in medium containing DMEM, 10% fetal calf serum, 2% pituitary extract and 4 μ M forskolin (Sigma-Aldrich, St Louis, MO). Schwann cells were then passaged upon reaching confluency in the same medium without forskolin. Schwann cells of passage 25 and higher were used in experiments unless otherwise indicated. When cells were to be treated with laminin (fragments or antibody) they were plated onto 16-well glass chamber slides (Nalgene Nunc, Rochester, NY) one day before the experiment at half-confluent density. The following day, the cells were incubated with laminins or other proteins at 37°C in DMEM/F12 containing 0.5% BSA.

Proteins and antibodies

EHS laminin-1, placental laminin-2/4 and collagen IV were purified as described (Cheng et al., 1997; Yurchenco and O'Rear, 1994). Laminin proteolytic fragments E3, E4, E8 and E1' were prepared as described (Yurchenco and O'Rear, 1994). Non-polymerizing laminin was prepared by treatment with AEBSF as described (Colognato et al., 1999). Rabbit polyclonal anti-laminin-1 antibody, anti-laminin-2/4 antibody, anti-E4 and anti-E8 antibodies against specific laminin proteolytic fragments were prepared by immunizing rabbits with the respective fragments. Each serum was affinity-purified on columns of immobilized fragment followed by cross-absorption against the other fragments as described (Yurchenco et al., 1993) and used at 10 μ g/ml. Rat monoclonal anti- γ 1 chain of laminin antibody were used at 1:125 dilution (Upstate Biotechnology Inc, Lake Placid, NY). Hamster β 1-integrin-specific IgM antibody Ha2/5 (BD Pharmingen, San Diego, CA) were used at a final concentration of 10 μ g/ml. Mouse monoclonal α -dystroglycan-specific antibody IIIH6 were used at a 1:2 dilution of HB101 hybridoma media (a kind gift of Kevin Campbell, University of Iowa). Monoclonal anti-Utrophin antibody (MANCHO3) were kindly provided by G. E. Morris (N. E. Wales Institute, UK) and were used at a 1:3 dilution for immunostaining. Monoclonal S100-specific antibody (DAKO Corp, Carpinteria, CA) were used at

1:100. Polyclonal goat anti-collagen type IV antibody were used at 1:100 (Southern Biotechnology, Birmingham, AL). FITC- and Cy3-conjugated secondary antibodies were from Sigma (St Louis, MO) and Jackson Immunochemicals (West Grove, PA) and were used as recommended.

Immunocytochemistry

Cells grown on 16-well slides, following various treatments, were rinsed three times with 10 mM sodium phosphate, pH 7.4, 127 mM NaCl (PBS, phosphate buffered saline), 0.5% bovine serum albumin (BSA) and fixed in 3% paraformaldehyde (EM Science, Gibbstown, NJ) in PBS for 10 minutes at room temperature. Cells were permeabilized 0.5% Triton X-100 in PBS, 0.5% BSA for 15 minutes on ice when staining of intracellular epitopes was desired. For detection of surface-bound or exposed proteins the detergent step was omitted with exception of Ha2/5 antibody. Blocking with 5% goat serum was performed for 30 minutes at room temperature. Cultures were then stained with various primary and appropriate secondary antibodies conjugated with either FITC or Cy3. All antibodies incubations were performed in PBS, 0.5% BSA, 0.5% goat serum for 1 hour at room temperature. Control staining was performed using standard primary IgG or IgM instead of specific ones. Slides were mounted in DAFCO mounting medium (Sigma-Aldrich) and imaged using an Olympus IX-70 inverted microscope fitted for epifluorescence and phase-contrast. Digital images were captured with a Princeton Instruments 5-mHz Micromax cooled-CCD camera fitted into the left side port.

Immunocytochemistry quantitation

Surface area covered by laminin or type IV collagen was calculated using IPLab 3.0 software. Seven random low magnification (20 \times) microscopic fields for each condition were photographed at the same exposure settings. A segmentation range was chosen based on immunofluorescence intensity and maintained for all conditions evaluated in the data set. Quantification of area coverage in the now highlighted segments was performed and normalized for the total cell area for each field.

Electron microscopy

Cells were plated onto 8-well Permanox chamber slides (Nalgene Nunc) 1 day before the experiment. Inhibiting agents (IIIH6 Ab, Ha2/5 Ab and laminin fragments) were added to cell cultures 20 minutes before the addition of 10 μ g/ml of laminin. Laminin, AEBSF-laminin and no laminin controls were performed in parallel. Cells adherent to plastic were fixed in 0.5% glutaraldehyde and 0.2% tannic acid in PBS for 1 hour at room temperature, and then transferred to modified Karnovsky's fixative (4% formaldehyde and 2.5% glutaraldehyde containing 8 mM CaCl₂ in 0.1 M sodium cacodylate buffer, pH 7.4). Samples were washed with PBS and post-fixed in 1% osmium tetroxide in 0.1 M sodium cacodylate buffer, pH 7.4 for 1 hour to produce osmium black. Samples were then dehydrated through a graded series of ethanol and embedded in Epon/SPURR resin (EM Science) that was polymerized at 65°C overnight. Both thick (1 μ m) and thin sections (~90 nm) were cut with a diamond knife on a Reichert-Jung Ultracut-E ultra-microtome. Thick sections were stained with 1% methylene blue in 1% sodium borate for light microscopy and thin sections were stained with saturated uranyl acetate (20 minutes) followed by 0.2% lead citrate (2.5 minutes). Images were photographed with a Jeol JEM-1200EX electron microscope.

To address the effect of blocking reagents on basement membrane, parameters were established to quantify the extent of electron-dense structures that formed on cell surfaces exposed to medium. Three different depth levels, separated by up to 1 mm, were cut into the cell

block for each sample to generate thin sections, with each thin section containing 5-10 cells. Fifteen electron micrographs were prepared for each level, taken randomly. The 45 micrographs from the same sample were randomly divided into three groups to permit determination of data scatter. Linear electron-dense (*lamina densa*) structures with a length of 2 μm and over were considered continuous. Short stretches of lamina densa-type matrix that were less than 2 μm in length were considered as discontinuous. Membrane surfaces lacking a recognizable *lamina densa* were considered as lacking recognizable surface-associated ECM. Data was expressed as the mean and standard deviation of the mean.

Flow cytometry analysis

Cells maintained at different passage numbers were seeded 1 day before the experiments in T75 flasks. For quantitative evaluation of the cell surface-bound laminin, cells were incubated with 10 $\mu\text{g}/\text{ml}$ of laminin-1 for 2 hours, washed with PBS and dissociated with cell dissociation buffer (Gibco BRL, Rockville, MD). Cell concentration was adjusted to 5×10^5 cells per ml. Suspended cells were blocked with 5% goat serum in PBS, 0.5% BSA and stained either with anti-laminin or anti-receptors antibodies diluted in washing buffer for 30 minutes. After washing with PBS, 0.5% BSA, 0.5% goat serum cells were incubated with appropriate secondary antibodies conjugated with FITC or Cy3 for 30 minutes. Following the last wash, cells were resuspended in 500 μl of PBS containing 0.5% BSA, 0.1% paraformaldehyde and analyzed by fluorescence-activated cell sorting (Epics-Profile II Coulter, Beckman Coulter, Fullerton, CA). Control experiments without primary antibody were performed in parallel.

Results

Primary Schwann cells have been observed to form basement membranes when co-cultured with dorsal root ganglion (DRG) neurons and fibroblasts but not when cultured alone, even if provided exogenous basement membrane components (Bunge et al., 1982). We found that cultured cells expressed little or no endogenous $\gamma 1$ -laminins or collagen type IV (as judged by immunostaining) regardless of passage. Furthermore, the ability of cultured Schwann cells to accumulate exogenous laminin-1 that covers substantial surface area and that possess ultrastructural characteristics of a basement membrane was dependent upon the cell state. In particular, the cells underwent a transition from a laminin incompetent to a competent state after passage-12. Except where indicated, cells were studied after this transition had occurred.

Exogenous laminin-1 and laminin-2 each form two distinct extracellular matrices on Schwann cell surfaces

To study Schwann cell-laminin interactions, we evaluated both mouse EHS laminin-1 ($\alpha 1\beta 1\gamma 1$) and human placental laminin-2/4 ($\alpha 2\beta 1\gamma 1$ and $\alpha 2\beta 2\gamma 1$). While $\alpha 2$ -laminins are major components found in developing and adult peripheral nerve basement membranes, laminin-1 is closely related, possesses many shared properties, and is more amenable to molecular dissection because of the availability of perturbing reagents. These laminins bear three full-length short arms and have been

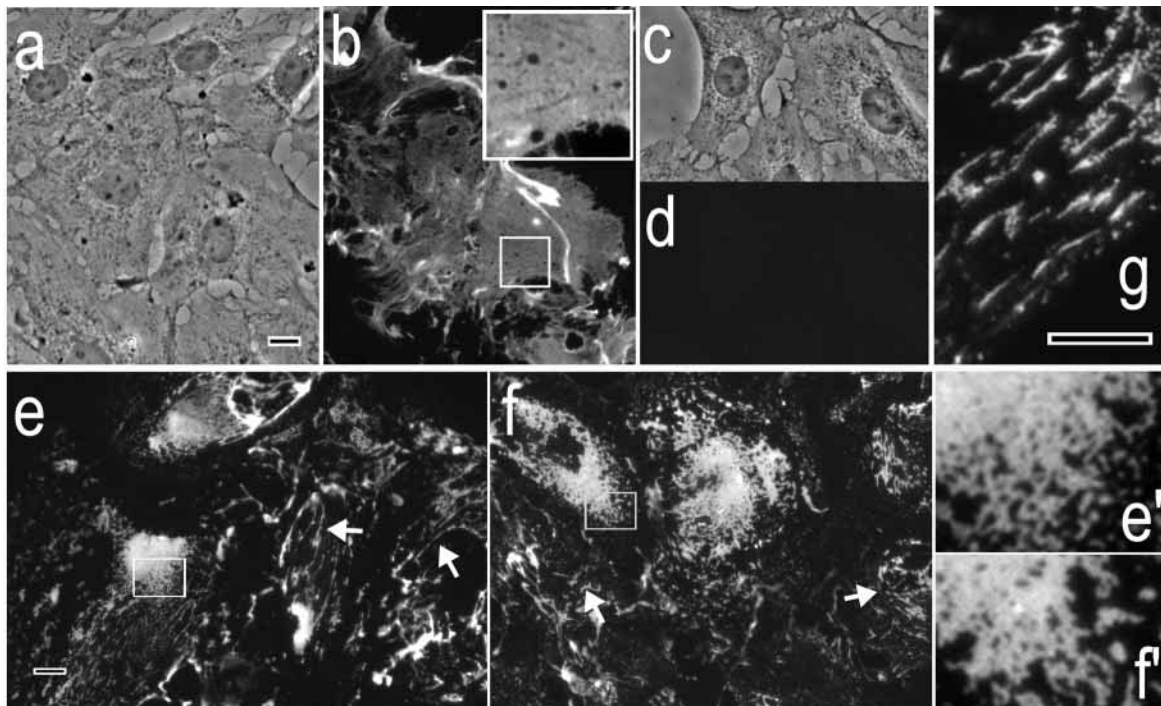


Fig. 1. Laminins assemble into two distinct extracellular matrices on Schwann cell surfaces. Laminin-1 and laminin-2/4 were each incubated with Schwann cells. Surface-bound laminin was visualized following fixation and immunostaining with anti-laminin primary and FITC-conjugated secondary antibodies. (a,b) Laminin-1 incubated with Schwann cells for 4 hours at 10 $\mu\text{g}/\text{ml}$ accumulated on cell surface showing dense reticular distribution. Insert shows higher magnification view of the boxed area. Phase image of the same field is shown. (c,d) Level of endogenous laminin was negligible. (e) Laminin-1 at lower concentration (2 $\mu\text{g}/\text{ml}$) showed less coverage with two distinct patterns clearly resolved: reticular (boxes) and fibrillar (arrows). (f) Laminin-2/4 assembled similar structures but had different concentration dependency. Shown is laminin-2/4 at 20 $\mu\text{g}/\text{ml}$. (e',f') High magnification view of boxed areas on e and f shown as examples of reticular pattern. Boxed areas are shown magnified in insets e' and f' to define the reticular pattern. (g) Example of a fibular structure is shown. Bars, 10 μm .

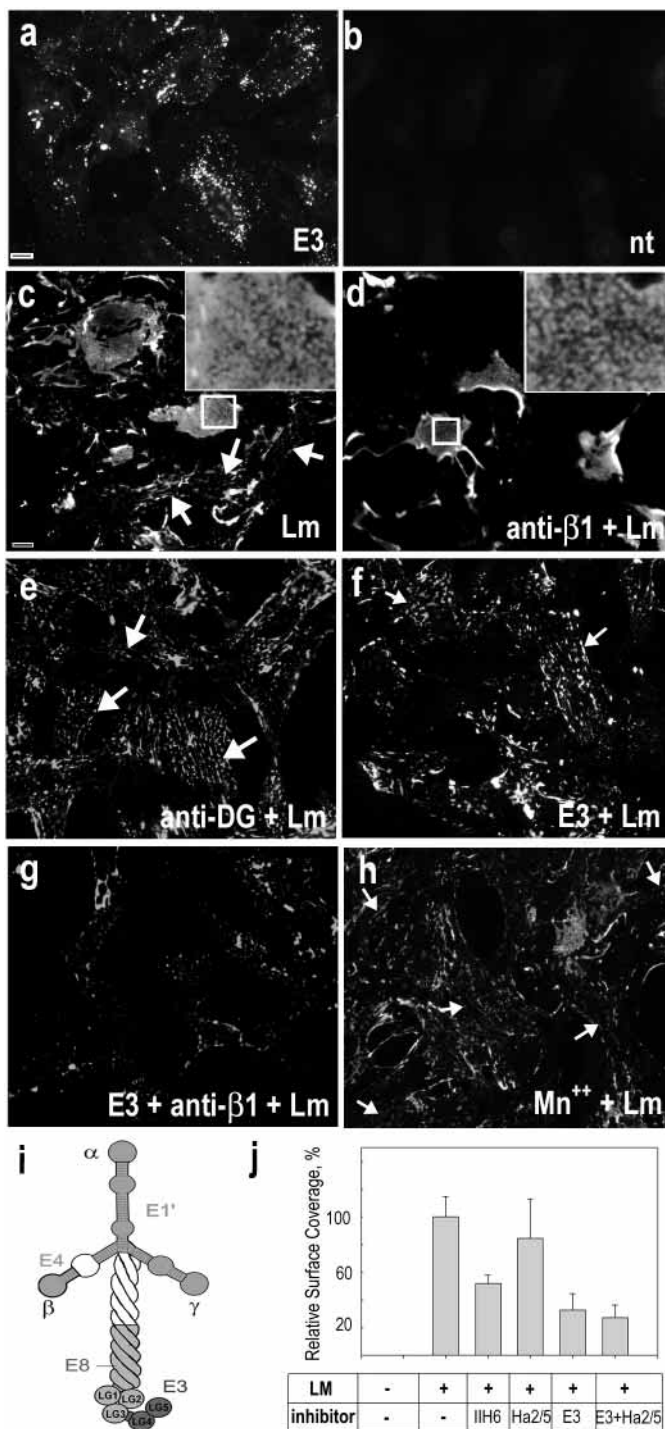
found to polymerize, interact with $\alpha 6\beta 1$, $\alpha 6\beta 4$ and $\alpha 1\beta 1$ integrins, and bind to dystroglycan.

Exogenous laminin-1 and laminins-2/4 were separately incubated with cultured Schwann cells in DMEM/F12 culture medium for 4 to 24 hours at 37°C. The resulting laminin surface patterns were detected by immunofluorescence microscopy following washing of cells to remove unbound components and paraformaldehyde fixation of cells in the absence of detergent. When Schwann cells were treated with exogenous laminin-1 (10 $\mu\text{g}/\text{ml}$) for 4 hours, extensive cell surface laminin coverage was detected by specific immunofluorescence (Fig. 1a,b). The pattern of staining changed little at longer incubation times (up to 24 hours). The level of endogenous laminin, as previously noted, was found to be negligible compared with exogenous laminin in these experiments (Fig. 1d). Schwann cells incubated with 2 $\mu\text{g}/\text{ml}$ of laminin-1 showed decreased cell surface accumulation of laminin with two distinct patterns of distribution. One pattern consisted of a dense plaque-like array referred to as the reticular pattern because at high magnification small cleared areas were detected in an otherwise confluent zone (Fig. 1e',f',e,f). This pattern was similar to the laminin-induced honeycombed pattern observed to form on cultured myotubes in the presence of exogenous laminin (Colognato et al., 1999). However, in Schwann cells the reticular mesh was denser with smaller intervening empty spaces within the array. At higher concentrations (10-20 $\mu\text{g}/\text{ml}$), laminin covered a larger fraction of the cell surface area becoming even denser with respect to size of the interstices of the array. The other architecture (fibrillar) consisted of longer narrow linear structures with limiting branching. (Fig. 1e,f, arrows, and g). The reticular matrix pattern predominated in terms of surface area coverage, particularly at higher laminin concentrations. Laminin-2/4 formed similar structures but had different concentration dependency. Subsequent

experiments focused on laminin-1 to permit evaluation with domain-specific reagents.

Selective inhibition of reticular and fibrillar matrices

Laminin domain, integrin and dystroglycan contributions to the cell surface accumulation of laminin-1 were evaluated (Fig. 2) with laminin fragments and receptor-blocking antibodies Ha2/5 (anti- $\beta 1$ -integrin), and IIH6 (anti- α -dystroglycan). Laminin-1 fragments E4 ($\beta 1$ short arm domains VI-V, 75 kDa), E1' (short arm complex excluding $\beta 1$ VI-IV, 450 kDa), E8



(lower half of coiled-coil with LG1-3, 200 kDa), and E3 (distal G-domain LG modules 4-5, 55 kDa) were incubated at 50 $\mu\text{g/ml}$ each in the absence of intact laminin for 4 hours with Schwann cells. Only fragment E3, which possesses both dystroglycan and heparin binding sites that map to LG4 (Sung et al., 1997; Talts et al., 1999), was detected on the cell surface following incubation. The binding was punctate in its appearance and less intense compared with intact laminin (Fig. 2a,b).

Laminin fragments E3, E8, E4 and E1' (50 $\mu\text{g/ml}$ each) were incubated with laminin-1 (2 $\mu\text{g/ml}$) and examined by immunofluorescence microscopy (Fig. 2). In addition, random images collected from low-magnification (20 \times) fields were analyzed to determine relative surface area coverage (Fig. 2j). Treatment of cells with β 1-integrin blocking antibody in the presence of laminin-1 prevented formation of nearly all fibrillar laminin structures, leaving the reticular structures largely intact (Fig. 2d). The addition of manganese, a divalent cation that enhances β 1-integrin binding (Gailit and Ruoslahti, 1988; Sonnenberg et al., 1988), increased the fraction of fibrillar matrix and decreased the fraction of reticular matrix (Fig. 2h). Fragment E3 had a significant inhibitory effect on laminin accumulation (65%), while the other fragments did not. The remaining bound laminin, following E3 inhibition, was noted to be almost exclusively in a fibrillar or dot-like distribution (Fig. 2f) (i.e. this fragment prevented the formation of the reticular pattern). The effect of IIH6 antibody was similar to E3 inhibition (Fig. 2e); however, overall, laminin inhibition was less (45%) and occasional small surviving reticular patches were observed. When E3 and anti- β 1 integrin antibody were incubated as a mixture with laminin, overall laminin surface binding was decreased only slightly beyond that achieved by E3 alone, however, both reticular and fibrillar patterns were observed to be almost entirely absent, with remaining laminin distributed into a punctate pattern (Fig. 2g). Somewhat surprisingly, interfering effects were not appreciated with other fragments at the concentrations used (Colognato et al., 1999). It is possible that E8 (an integrin-binding fragment) may not have blocked fibrillar anchorage due to integrin contributions arising from other domains, while E1', which cannot directly interact with the cell surface, may not have blocked matrix assembly because of a very high surface concentration of laminin.

Contributions of laminin polymerization

Both α 1- and α 2-laminins polymerize to form network structures that contribute a non-collagenous superstructure of basement membranes containing these laminins (Cheng et al., 1997; Yurchenco and Cheng, 1993; Yurchenco et al., 1992). Amino ethyl benzene sulfonyl fluoride (AEBSF) covalently binds to the short arms of polymerizing laminin, selectively abolishing polymerization without affecting cell adhesion, heparin binding, or dystroglycan binding (Colognato et al., 1999). When Schwann cells were incubated with non-polymerizing-laminin (both 5 $\mu\text{g/ml}$), the laminin was noted to still bind to the cell surface (Fig. 3). However, the surface density was lower and more evenly distributed, and the recognizable reticular architecture was greatly diminished.

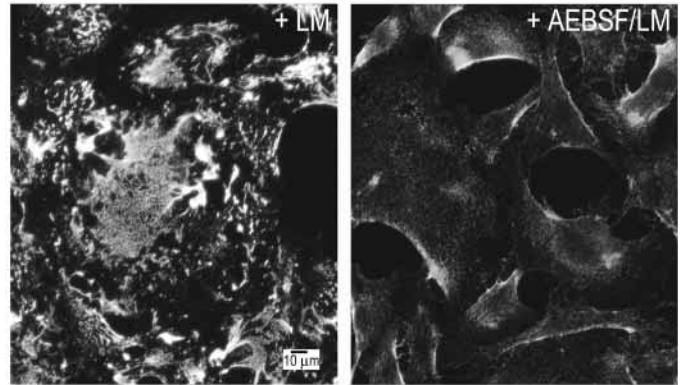


Fig. 3. Cell surface binding of non-polymerizing laminin-1. Laminin-1, untreated (+LM, left panel) or treated with AEBSF to selectively inhibit polymerization (+AEBSF-LM), were incubated at 5 $\mu\text{g/ml}$ for 4 hours with Schwann cells. The cell surface distribution of laminin-1 was determined by immunofluorescence microscopy. Non-polymerizing laminin bound to the cell surface with a diffuse distribution.

Topographical associations of laminin-1 with dystroglycan and integrin receptors

Schwann cells, untreated or incubated for 8 hours with laminin-1 (2 $\mu\text{g/ml}$), were immunostained to detect both laminin and α -dystroglycan (Fig. 4). The pattern of untreated cells was noted to be that of a dense and coarse punctate distribution of dystroglycan epitopes across the entire exposed cell surface. After laminin treatment, the pattern was now observed to be plaque-like, consisting of more densely packed but finer dots, concentrated in zones of the exposed cell surface. These dystroglycan zones co-localized with those decorated by laminin in the reticular matrix. Following laminin incubation in the presence of β 1-integrin-blocking antibody, the fibrillar component was observed to be absent without affecting the reticular laminin structures.

The integrin was found, in the absence of exogenous laminin, to be widely distributed as a fibrillar-like mesh (Fig. 5). Following an 8-hour treatment with laminin-1 the integrin pattern remained largely unchanged. Laminin within the fibrillar array was noted to correspond to a subset of the β 1-integrin fibrils [i.e. the laminin fibrils co-localized with only some of the integrin-staining fibrils (arrows)]. By contrast, no co-localization of reticular laminin patterns with integrin was identified. Although it is possible that the particular integrin fibrils that co-localized with laminin were induced to assemble in an otherwise pre-existing integrin array, the similarity of structures before and after laminin treatment were too great to be able to make such a distinction. In the presence of E3, which blocked formation of the reticular structure, the remaining fibrillar laminin co-distributed with a subset of integrin fibrils.

Effect of laminin matrix assembly on the distribution of cytoskeletal proteins

To determine whether laminin-dependent matrix assembly induced a rearrangement of cytoskeletal partners known to interact with dystroglycan and integrins, we evaluated the distributions of utrophin, vinculin and paxillin before and after treatment of Schwann cells with laminin (Fig. 6). Utrophin, the

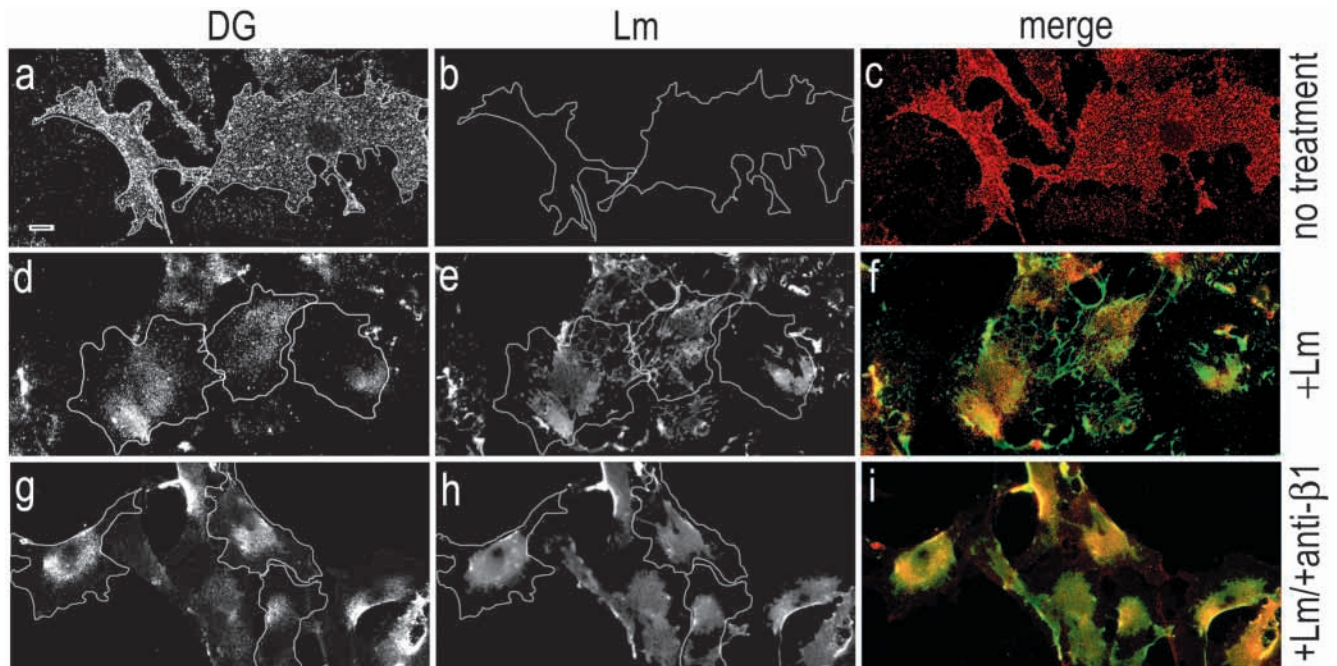


Fig. 4. Dystroglycan topography in response to laminin-1. Schwann cells were incubated with 2 $\mu\text{g}/\text{ml}$ of laminin-1 for 8 hours with (g,h,i) and without (d,e,f) anti- $\beta 1$ integrin blocking antibody. Schwann cells incubated in the same media but without exogenous laminin-1 shown as control (a,b,c). Non-permeabilizing fixation conditions were used. (a,b,c) In the absence of laminin, dystroglycan was distributed along the Schwann cell surface in a fine punctuate pattern. The level of endogenous laminin immunostaining was negligible. (d,e,f) Surface dystroglycan was observed to be distributed into focal areas on cell surface following 8 hours of incubation with laminin-1. Cell borders are indicated with lines (determined from the corresponding phase images) to aid in the analysis of dystroglycan rearrangement. Laminin distribution from the corresponding area is shown. Merged image reveals zonal co-localization of dystroglycan with the reticular structures of laminin. (g,h,i) In the presence of $\beta 1$ -integrin blocking antibody, which blocks formation of fibrillar matrix, laminin and dystroglycan co-localization is now seen almost exclusively within plaque-like reticular matrices. Bar, 10 μm .

peripheral nerve homologue of dystrophin that binds to dystroglycan (Yamada et al., 1996), was distributed in a diffuse punctate pattern similar to that noted for dystroglycan. Following overnight incubation with laminin, utrophin was noted to be distributed into a more condensed pattern whose borders corresponded to those of laminin reticular structures (Fig. 6b,c). Vinculin and paxillin are two cytoskeletal

components found in association with $\beta 1$ -integrin in focal adhesions. These components were not observed to be associated with either the reticular or fibrillar matrices (Fig. 6d-g). Regardless of laminin treatment, vinculin and paxillin were found to be present only with the plasma membrane attached to the plastic surface (i.e. they were on a focal plane below that of the two matrices) and were not altered in their apparent distribution or number in response to added laminin.

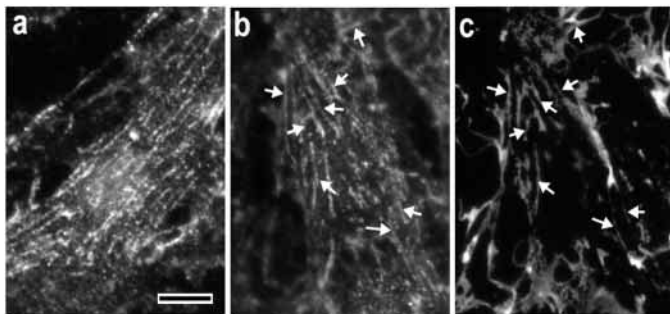


Fig. 5. Distribution of $\beta 1$ -integrin in the absence and presence of laminin. Cells were incubated with 2 $\mu\text{g}/\text{ml}$ of laminin for 8 hours. Cells were fixed, immunostained with laminin-specific antibody, then permeabilized with Triton X-100 and co-stained with anti- $\beta 1$ integrin antibody. (a) $\beta 1$ -integrin was distributed in fibrillar arrays prior to treatment with laminin. Panels b and c reveal integrin and laminin within the same field. Following laminin incubation, co-localization on a subset of integrin fibrils with laminin (arrows indicate examples) was observed. Bar, 10 μm .

Laminin-1 induction of an ultrastructural basement membrane morphology

Schwann cells were incubated with laminin-1 (20 $\mu\text{g}/\text{ml}$) for 8 hours, fixed and prepared for electron microscopy (Fig. 7). The sections were cut orthogonal to the plane of the plastic to enable visualization of the plasma membrane that faced the media environment. In the absence of exogenous laminin, this outer surface lacked discernable extracellular matrix (Fig. 7a,C). Following treatment with laminin-1, the outer plasma membrane surface was noted to be covered by a linear extracellular matrix. This ECM appeared as a thin continuous electron-dense line overlying a more lucent zone, measuring 20-40 nm in overall thickness (Fig. 7a,A). This ultrastructural morphology was that of a *lamina densa* and *lamina lucida*, respectively, and was considered the typical ultrastructural morphology of a thin basement membrane. Although long stretches of basement membrane were detected, some sections revealed discontinuities or portions of absent matrix as would

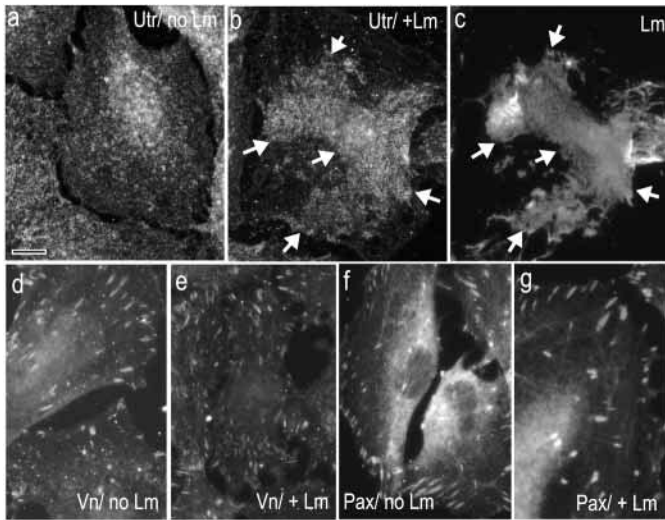
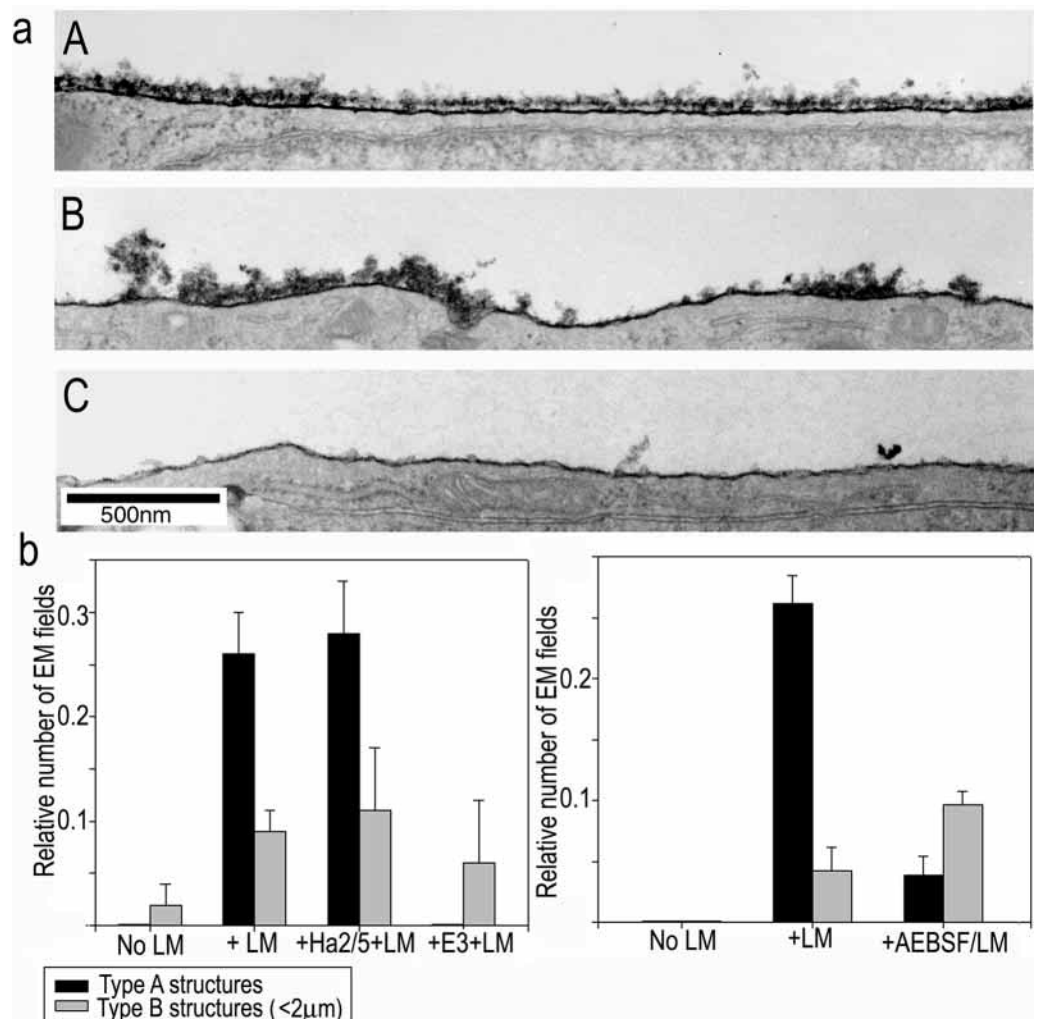


Fig. 6. Distributions of cytoskeletal components. Laminin at 5 mg/ml was incubated with Schwann cells for 18 hours. Effect of laminin cell surface assembly on several cytoskeletal proteins was evaluated. (a-c) The distribution of utrophin was detected with monoclonal antibody MANCHO3 with and without laminin treatment. Utrophin reorganization was noted with laminin treatment (compare a and b, border shown with arrows). Laminin-utrophin co-localizations were noted after 18 hours of laminin incubation. (d-g) Vinculin (Vn; d,e) and paxillin (Pax; f,g) were noted to be present on the cell/plastic interface; neither co-localized with a laminin matrix. Bar, 10 μ m

be expected given less than complete surface coverage by laminin as was shown by immunostaining of the parallel cultures under same conditions (Fig. 7a,B).

Fig. 7. (a) Electron microscopy. Schwann cells were incubated with and without 10 μ g/ml of laminin-1 for 18 hours. In addition, cells incubated with laminin were treated with E3 fragment or blocking antibodies. Three types of cell membrane-associated ECM were detected: continuous electron-dense cell surface associated structure (*lamina densa*, frame A, >2 μ m); or short stretches of electron-dense matrix (frame B, <2 μ m); cells cultured without laminin revealed a matrix-free plasma membrane surface (frame C), with infrequent small amorphous deposits such as that in the middle of frame C. By contrast, cells incubated with laminin showed the presence of a *lamina densa*. Inhibition of laminin- β 1-integrin interaction by antibody Ha2/5 (50 μ g/ml) did not abolish the appearance of a membrane-associated electron dense structure. Fragment E3 (100 μ g/ml), in contrast to β 1-integrin blocking antibody, prevented formation of an electron dense structure. Bar, 500 nm.

(b) Quantitation of morphology. The distribution of non-polymerizable laminin and its ability to induce a membrane-associated electron dense structure was analyzed after 8 hours of incubation with 10 μ g/ml of polymerizing or AEBSF-laminin-1. Non-polymerizing laminin generated little continuous matrix. The graph shows the relative number of events according to analysis of three random cross-sections, as described in Materials and Methods.



Blocking experiments with agents that interfere with laminin surface accumulation was performed in order to evaluate their effect on the appearance of an electron-dense extracellular matrix. After overnight incubation with 10 μ g/ml of laminin-1 with or without blocking antibodies or fragments, cells were prepared for electron microscopy or for the control immunostaining. The *lamina densa* was judged to be continuous if it extended for a uninterrupted length of 2 μ m or greater and discontinuous if it extended for less than that length (Fig. 7a). Formation of a *lamina densa*, either continuous or discontinuous, was prevented by a molar excess of fragment

E3, a selective inhibitor of reticular matrix (Fig. 7b, left panel). By contrast, β 1-integrin blocking antibody, a selective inhibitor of fibrillar matrix, did not prevent formation of a continuous *lamina densa*. Thus there is a correlation between the reticular matrix and ultrastructural basement membrane morphology in which E3 inhibits the formation of both.

Role of laminin polymerization at the ultrastructural level

Treatment of Schwann cells with the non-polymerizing laminin (AEBSF-treated) resulted in a substantially altered distribution and significant reduction of laminin surface coverage by light immunomicroscopy as previously noted (Fig. 3). Electron microscopy was performed on cell samples incubated either with laminin-1 or non-polymerizing laminin-1, both at 10 μ g/ml for 18 hours. A substantial decrease of a continuous *lamina densa* was noted with partial shift to the discontinuous form (Fig. 7b, graph).

Type IV collagen contributions

Basement membrane formed with laminin alone was considered to be a nascent ECM in that it lacked type IV collagen, a major structural component of mature basement membranes. No immuno-reactive type IV collagen was detected on Schwann cell surfaces either before or after laminin treatment alone (Fig. 8). However, if exogenous type IV collagen was added to cultures, or if endogenous type IV collagen secretion was promoted with L-ascorbic acid (which stabilizes collagen triple-helix structure and which has been previously shown to cause collagen deposition (Chernousov et al., 1998)), collagen type IV was then observed to accumulate on cell surfaces (Fig. 8 and data not shown). This collagen was present either in fibrillar structures or small, amorphous, brightly immunostaining particles. However, type IV collagen did not accumulate into recognizable reticular patterns without added laminin. To determine whether collagen type IV would associate with the reticular laminin, the collagen (50 μ g/ml) was incubated with laminin-1 (5 μ g/ml) for 8 hours. The two proteins were observed to be co-localized in both the reticular and fibrillar matrices.

When Schwann cells were incubated with type IV collagen in the presence of β 1 integrin-blocking antibody, it was no longer detected on the cell surface (Fig. 9). Thus, it appears likely that all type IV collagen surface accumulation is integrin-dependent in the absence of laminin. To study laminin-dependent component of collagen assembly we blocked β 1-integrin and examined type IV collagen accumulation in the presence of laminin (Fig. 9). Under these conditions, type IV collagen was detected only in laminin-containing reticular plaques. Thus, the nascent laminin-based basement membranes were competent to incorporate type IV collagen.

Schwann cell laminin-binding competency and expression of dystroglycan and integrin as a function of cell passage

Schwann cell laminin-binding competency was found to be dependent on the passage number. Low-passage cells (LPC; below 12) exhibited only a limited coverage by laminin, nearly all in a fibrillar pattern, whereas high-passage cells (HPC, >25)

accumulated significantly higher amounts of laminin predominately in the reticular pattern (Fig. 10a,b). Schwann cells retained expression of the differentiation marker S100 in both low and high passage cells (Fig. 10c). FACS analysis was used to evaluate the relative amount of laminin-1 (incubated at 10 μ g/ml for 2 hours) that could bind Schwann cell surfaces (Fig. 10d). Substantially higher (about 200-fold) surface laminin-1 was noted in HPC compared with LPC to the HPC. This result suggests that Schwann cells undergo a differentiation during passaging that involves the expression of one or more critical laminin cell surface anchors, enabling basement membrane formation.

To address this, the relative levels of cell surface β 1-integrin and α -dystroglycan on LPC and HPC were examined by flow cytometry (Fig. 10e,f). Surprisingly, the dystroglycan level remained essentially the same with β 1-integrin only about twofold higher in the HPC. Such a difference in β 1-integrin would not account for the greater than 100-fold overall laminin increase and in any case is not expected to be relevant for

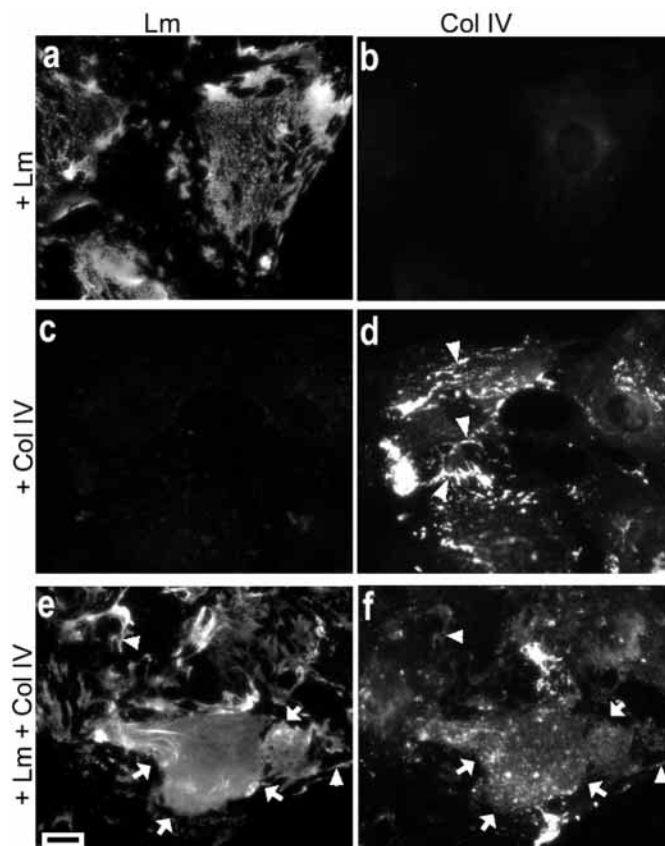


Fig. 8. Contributions of type IV collagen. EHS type IV collagen was incubated with Schwann cells for 4 hours with or without laminin. Cells were washed, fixed and double-stained with anti-laminin (a,c,e) and anti-collagen type IV (b,d,f) antibodies and corresponding Cy3- or FITC-conjugated secondary antibodies. Accumulation of exogenous laminin on the cell surface occurred without the presence of type IV collagen (a). Exogenous type IV collagen accumulated on the cell surface (d,f), even in the absence of laminin (d), forming mostly fibrillar structures (arrowheads). In the presence of laminin, exogenous type IV collagen also assembled into the reticular type of pattern (f, arrows, compare laminin in e). Bar, 10 μ m.

basement membrane coverage. Therefore the increased laminin accumulation on the surface of high passage Schwann cells could not be explained simply by change in expression of these laminin receptors. This suggests the existence of a third anchoring component important for laminin assembly. Heparin/sulfatide binding is the other major binding activity that maps to E3, the inhibiting fragment (Talts et al., 1999). A cell surface heparan sulfate proteoglycan, or possibly a sulfatide, might correspond to this anchor. Heparin (0.1 mg/ml), was found to eliminate most of the laminin distributed in a reticular pattern (data not shown), supporting this possibility.

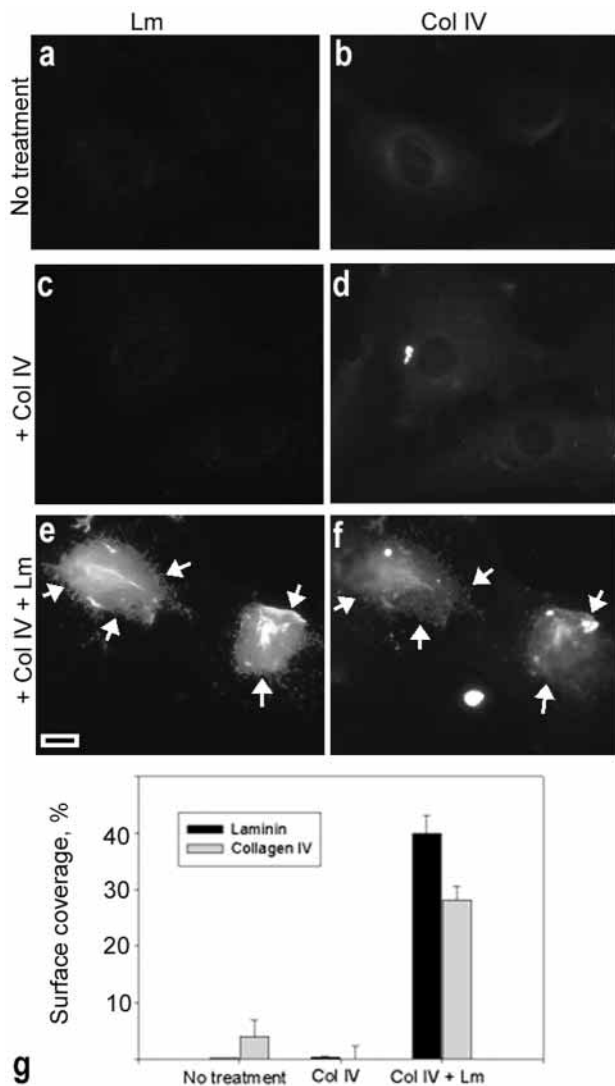


Fig. 9. Laminin-dependent type IV collagen assembly. Cells were either untreated (a,b) or incubated with type IV collagen with (e,f) or without (c,d) laminin in the presence of anti- $\beta 1$ blocking antibody (all panels), which prevents the formation of fibrillar structures. Cells were fixed and stained as described in Fig. 8. In the absence of laminin, type IV collagen did not accumulate on the cell surface (d). In the presence of laminin, type IV collagen assembled into reticular structures (f) that co-localized with those of laminin (e). Bar, 10 μ m. (g) The graph compares surface coverage by type IV collagen (gray) or laminin (black) with or without exogenous laminin.

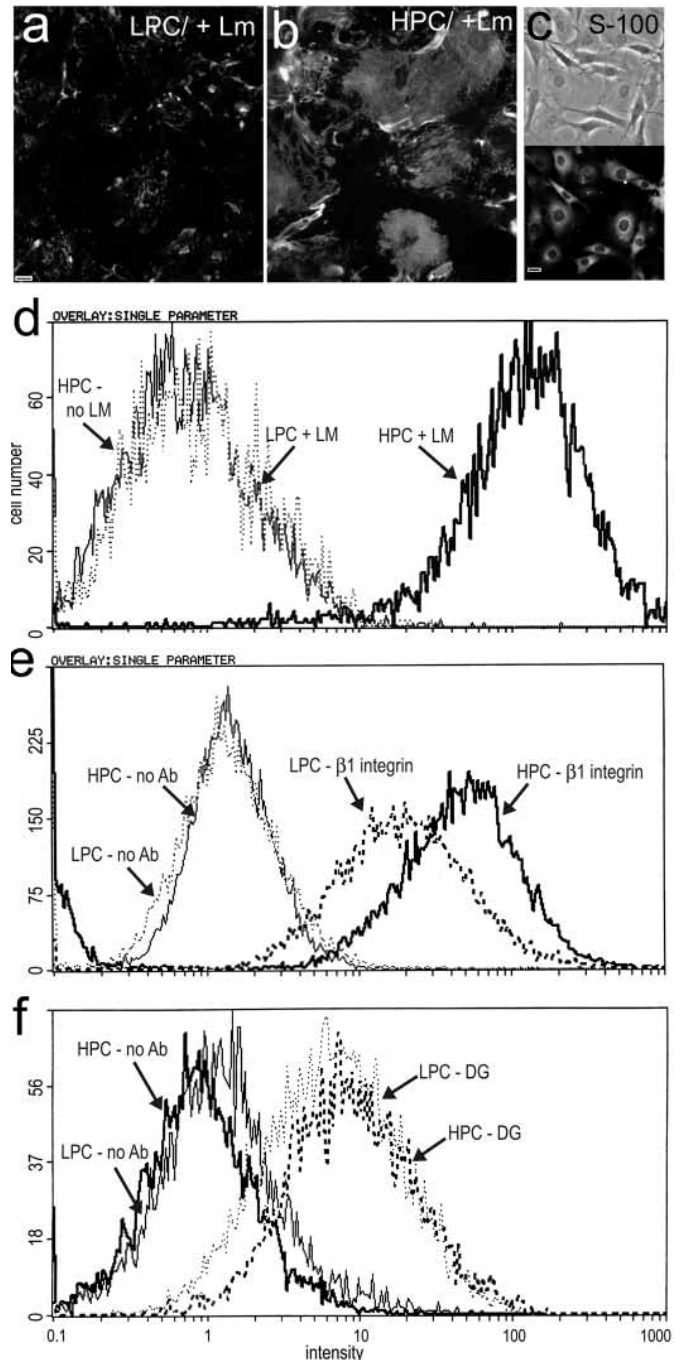


Fig. 10. Schwann cell passage-dependency of laminin binding capacity and receptor expression. Laminin (10 μ g/ml) was incubated in serum-free culture medium with high-passage (HPC, P27) and low-passage (LPC, P12) Schwann cells for 2 hours. Cell surface-bound laminin was visualized by immunofluorescence microscopy with laminin-specific antibody (a,b) and analyzed by flow cytometry (e, thick line shows the distribution of cell surface-bound laminin intensities for HPC, while the thin solid line is the distribution for the LPC). The level of laminin bound to the cell surface of HPC was more than 100-times higher than that bound to LPC. Flow cytometry of $\beta 1$ -integrin (e) and α -dystroglycan (f) reveal that $\beta 1$ -integrin levels are about threefold higher in HPC, whereas α -dystroglycan levels remain nearly the same in HPC and LPC. High-passaged cells continue to express the Schwann cell-specific marker S-100 (e). Bar, 10 μ m (a-d).

Discussion

Schwann cell basement membranes do not appear to form in developing tissues until the stage of neuronal ensheathment, and it has been postulated that axonal contact triggers their assembly, in turn affecting cell polarization, ensheathment and myelination (Clark and Bunge, 1989; Jaakkola et al., 1993). The data presented in this study suggest that Schwann cell basement membrane assembly is a process that first requires the development of cell surface competency for laminin binding, followed by the binding and assembly of laminin. We consider this ECM as a 'nascent' basement membrane (i.e. a laminin-based ECM with classical ultrastructural morphology of a basement membrane, but still lacking in type IV collagen). The nascent basement membrane is likely to be no more than one laminin molecular layer thick. Upon exposure of the cells to type IV collagen, this component is incorporated into the laminin matrix. In Schwann cells, the laminin binding/assembly step depends in part upon an interaction of laminin with α -dystroglycan. In response to laminin surface accumulation, dystroglycan and its cytoskeletal partner utrophin redistribute on the cell surface into a condensed topographical organization that corresponds to that formed by laminin in a polymerization-dependent manner. Surprisingly, formation of this structure, which corresponded by light immunomicroscopy to the dense reticular array, was not found to require interaction with β 1-integrin.

Laminin and type IV collagen have been found to possess the intrinsic and separate ability to polymerize, contributing the two major known architectural networks of basement membranes (Yurchenco, 1994; Yurchenco et al., 1992; Yurchenco and Furthmayr, 1984). However, these protein characteristics, in themselves, were found to be insufficient to insure the formation of a cell-based ECM. An additional critical factor appears to be that of cell anchorage. For such assembly to occur on Schwann cells, the cells had to be in a competent state for laminin binding. Low passage cells bound laminin to a very limited degree with such laminin detected in fibrillar-like arrays but not nascent basement membranes. By contrast, cells at later passage became capable of binding laminin with over a 100-fold higher capacity. Addition of laminin to these cells initiated assembly of nascent basement membranes that predominated over the fibrillar matrix in terms of surface coverage. Nascent basement membrane, enabled by competency and triggered with exogenous laminin, required surface binding through laminin LG modules 4-5 located in the large globular domain at the end of the long arm. It seems likely that it is this binding interaction that is rendered permissive through cell-passaging. In comparing incompetent and competent laminin-binding cells, no difference was detected in cell surface dystroglycan and little difference was detected in β 1-integrin. This surprising finding suggests that an additional cell surface anchor for LG4-5 is either expressed or activated as the cell becomes competent. Given that heparin/heparan sulfate binding is the other major activity identified in E3 (mediated by LG module-4), surface anchorage may depend upon a cell surface-associated heparan sulfate proteoglycan (HSPG). Consistent with this consideration, we have found that heparin inhibits the accumulation of both laminin-1 and laminins-2/4 into nascent basement membrane. Although dystroglycan binding is in itself inhibited by heparin in the case of laminin-1, this is not the case with laminin-2 (Pall et al., 1996) and therefore not likely to be

dependent on dystroglycan alone. It is also possible that an anchoring contribution could be provided by sulfated glycolipid (sulfatide) that bind to the heparin sequences (Roberts et al., 1985; Talts et al., 1999). The putative surface anchor, if a HSPG, is likely to be linked to the dystroglycan interaction, perhaps acting as a 'co-receptor', given the finding that dystroglycan and heparin binding sequences are located on the same LG-4 protein face (Tisi et al., 2000). We suggest that the phenotypic switch thought to occur in Schwann cells upon neuronal contact may involve this anchoring state passage-dependent transition, a requirement over and above a separate requirement for the initiation of the synthesis of basement membrane components. Given that Schwann cells undergo a developmental transition from individual cells to ones that envelop axons and produce an abaxonal basement membrane, what might be the functional role of the fibrillar matrix? Its structural topography is similar to that of the integrin-associated fibrillar architecture induced by fibronectin on fibroblasts, cells that cannot form basement membranes (Klass et al., 2000; Zhong et al., 1998). The fibrillar matrix in Schwann cells might have a function important for migration and neuronal growth-cone pathfinding in the stages that precede envelopment and that occurs both in nerve development and regeneration.

The characteristics of Schwann cell basement membrane assembly were related to those observed on myotubes (Colognato et al., 1999) in that both showed a selective E3-dependency and were inhibited with dystroglycan blocking antibody, but not by integrin blocking antibody. Both also showed a dependency on laminin polymerization with the greatest contribution seen in myotubes. A substantial difference was seen in the co-localization of laminin with integrin and vinculin in the case of myotubes, and its lack in Schwann cells. Thus, the receptor and cytoskeletal partners associated with laminin can differ under different circumstances, suggesting that they could be found to be cell-type specific. In Schwann cells, the fibrillar matrix was not associated with an ultrastructurally defined basement membrane, although it did associate with type IV collagen. Therefore, this distinct ECM, discontinuous in its distribution, appears to be a unique entity. Similar structures have been identified on Schwann cells previously, and our data are in agreement with the conclusion that these ECMs are not precursor to basement membrane (Chernousov and Carey, 2000; Chernousov et al., 1998). Given the ability of basement membrane-incompetent Schwann cells to assemble these matrices, and given their resemblance to fibrillar matrices seen on fibroblasts, these ECMs might be primarily attributes of a variety of migrating cells that are not involved in the process of basement membrane assembly.

The factors that determine which cell surfaces can host basement membranes have been unexplained in the past. Muscle and fat cells become enveloped by these ECMs while epithelial cells develop a basement membrane restricted to their abluminal surface. Fibroblasts, even though they secrete basement membrane components, do not assemble their own basement membranes. The data from this study argue for the existence of a laminin G-domain interacting, integrin-independent anchoring complex that imparts competency for basement membrane assembly and that is to be distinguished from receptors that mediate fibrillar matrix. Future goals will be to elucidate cell surface molecules and their cytoskeletal

partners that constitute the complex and to determine the mechanisms that differentially drive ECM assembly and mediate functions.

This study was supported by grants (DK36425 and NS38469) from the National Institutes of Health. We thank Raj Patel (Robert W. Johnson Medical School) for the preparation of samples for electron microscopy.

References

- Brakebusch, C., Grose, R., Quondamatteo, F., Ramirez, A., Jorcano, J. L., Pirro, A., Svensson, M., Herken, R., Sasaki, T., Timpl, R., Werner, S. and Fassler, R. (2000). Skin and hair follicle integrity is crucially dependent on beta1 integrin expression on keratinocytes. *EMBO J.* **19**, 3990-4003.
- Bunge, M. B., Williams, A. K. and Wood, P. M. (1982). Neuron-Schwann cell interaction in basal lamina formation. *Dev. Biol.* **133**, 393-404.
- Cheng, Y. S., Champliaud, M. F., Burgeson, R. E., Marinkovich, M. P. and Yurchenco, P. D. (1997). Self-assembly of laminin isoforms. *J. Biol. Chem.* **272**, 31525-31532.
- Chernousov, M. A. and Carey, D. J. (2000). Schwann cell extracellular matrix molecules and their receptors. *Histol. Histopathol.* **15**, 593-601.
- Chernousov, M. A., Stahl, R. C. and Carey, D. J. (1998). Schwann cells use a novel collagen-dependent mechanism for fibronectin fibril assembly. *J. Cell Sci.* **111**, 2763-2777.
- Clark, M. B. and Bunge, M. B. (1989). Cultured Schwann cells assemble normal-appearing basal lamina only when they ensheath axons. *Dev. Biol.* **133**, 393-404.
- Colognato, H. and Yurchenco, P. D. (1999). The laminin alpha2 expressed by dystrophic dy(2J) mice is defective in its ability to form polymers. *Curr. Biol.* **9**, 1327-1330.
- Colognato, H. and Yurchenco, P. D. (2000). Form and function: the laminin family of heterotrimers. *Dev. Dyn.* **218**, 213-234.
- Colognato, H., MacCarrick, M., O'Rear, J. J. and Yurchenco, P. D. (1997). The laminin alpha2-chain short arm mediates cell adhesion through both the alpha1beta1 and alpha2beta1 integrins. *J. Biol. Chem.* **272**, 29330-29336.
- Colognato, H., Winkelmann, D. A. and Yurchenco, P. D. (1999). Laminin polymerization induces a receptor-cytoskeleton network. *J. Cell Biol.* **145**, 619-631.
- Cote, P. D., Moukhles, H., Lindenbaum, M. and Carbonetto, S. (1999). Chimeric mice deficient in dystroglycans develop muscular dystrophy and have disrupted myoneural synapses. *Nat. Genetics* **23**, 338-342.
- DiPersio, C. M., Hodivala-Dilke, K. M., Jaenisch, R., Kreidberg, J. A. and Hynes, R. O. (1997). alpha3beta1 integrin is required for normal development of the epidermal basement membrane. *J. Cell Biol.* **137**, 729-742.
- Einheber, S., Milner, T. A., Giancotti, F. and Salzer, J. L. (1993). Axonal regulation of Schwann cell integrin expression suggests a role for alpha 6 beta 4 in myelination. *J. Cell Biol.* **123**, 1223-1236.
- Fernandez-Valle, C., Gwynn, L., Wood, P. M., Carbonetto, S. and Bunge, M. B. (1994). Anti-beta 1 integrin antibody inhibits Schwann cell myelination. *J. Neurobiol.* **25**, 1207-1226.
- Gailit, J. and Ruoslahti, E. (1988). Regulation of the fibronectin receptor affinity by divalent cations. *J. Biol. Chem.* **263**, 12927-12932.
- Guicheney, P., Vignier, N., Helbling-Leclerc, A., Nissinen, M., Zhang, X., Cruaud, C., Lambert, J. C., Richelme, C., Topaloglu, H., Merlini, L. et al. (1997). Genetics of laminin alpha 2 chain (or merosin) deficient congenital muscular dystrophy: from identification of mutations to prenatal diagnosis. *Neuromusc. Disord.* **7**, 180-186.
- Henry, M. D. and Campbell, K. P. (1996). Dystroglycan: an extracellular matrix receptor linked to the cytoskeleton. *Curr. Opin. Cell Biol.* **8**, 625-631.
- Henry, M. D. and Campbell, K. P. (1998). A role for dystroglycan in basement membrane assembly. *Cell* **95**, 859-870.
- Jaakkola, S., Savunen, O., Halme, T., Uitto, J. and Peltonen, J. (1993). Basement membranes during development of human nerve: Schwann cells and perineurial cells display marked changes in their expression profiles for laminin subunits and beta 1 and beta 4 integrins. *J. Neurocytol.* **22**, 215-230.
- Klass, C. M., Couchman, J. R. and Woods, A. (2000). Control of extracellular matrix assembly by syndecan-2 proteoglycan. *J. Cell Sci.* **113**, 493-506.
- Kuang, W., Xu, H., Vachon, P. H., Liu, L., Loechel, F., Wewer, U. M. and Engvall, E. (1998). Merosin-deficient Congenital Muscular Dystrophy. Partial genetic correction in two mouse models. *J. Clin. Invest.* **102**, 844-852.
- Lohikangas, L., Gullberg, D. and Johansson, S. (2001). Assembly of laminin polymers is dependent on beta1-integrins. *Exp. Cell Res.* **265**, 135-144.
- Matsumura, K., Yamada, H., Saito, F., Sunada, Y. and Shimizu, T. (1997). Peripheral nerve involvement in merosin-deficient congenital muscular dystrophy and dy mouse. *Neuromusc. Disord.* **7**, 7-12.
- Pall, E. A., Bolton, K. M. and Ervasti, J. M. (1996). Differential heparin inhibition of skeletal muscle alpha-dystroglycan binding to laminins. *J. Biol. Chem.* **271**, 3817-3821.
- Patton, B. L., Miner, J. H., Chiu, A. Y. and Sanes, J. R. (1997). Distribution and function of laminins in the neuromuscular system of developing, adult, and mutant mice. *J. Cell Biol.* **139**, 1507-1521.
- Roberts, D. D., Rao, C. N., Magnani, J. L., Spitalnik, S. L., Liotta, L. A. and Ginsburg, V. (1985). Laminin binds specifically to sulfated glycolipids. *Proc. Natl. Acad. Sci. USA* **82**, 1306-1310.
- Sasaki, T., Forsberg, E., Bloch, W., Addicks, K., Fassler, R. and Timpl, R. (1998). Deficiency of beta 1 integrins in teratoma interferes with basement membrane assembly and laminin-1 expression. *Exp. Cell Res.* **238**, 70-81.
- Shorer, Z., Philpot, J., Muntoni, F., Sewry, C. and Dubowitz, V. (1995). Demyelinating peripheral neuropathy in merosin-deficient congenital muscular dystrophy. *J. Child Neurol.* **10**, 472-475.
- Sonnenberg, A., Modderman, P. W. and Hogervorst, F. (1988). Laminin receptor on platelets is the integrin VLA-6. *Nature* **336**, 487-489.
- Stewart, H. J., Turner, D., Jessen, K. R. and Mirsky, R. (1997). Expression and regulation of alpha1beta1 integrin in Schwann cells. *J. Neurobiol.* **33**, 914-928.
- Sunada, Y., Bernier, S. M., Utani, A., Yamada, Y. and Campbell, K. P. (1995). Identification of a novel mutant transcript of laminin alpha 2 chain gene responsible for muscular dystrophy and dysmyelination in dy2J mice. *Hum. Mol. Genet.* **4**, 1055-1061.
- Sung, U., O'Rear, J. J. and Yurchenco, P. D. (1997). Localization of heparin binding activity in recombinant laminin G domain. *Eur. J. Biochem.* **250**, 138-143.
- Talts, J. F., Andac, Z., Gohring, W., Brancaccio, A. and Timpl, R. (1999). Binding of the G domains of laminin alpha1 and alpha2 chains and perlecan to heparin, sulfatides, alpha-dystroglycan and several extracellular matrix proteins. *EMBO J.* **18**, 863-870.
- Tisi, D., Talts, J. F., Timpl, R. and Hohenester, E. (2000). Structure of the C-terminal laminin G-like domain pair of the laminin alpha2 chain harbouring binding sites for alpha-dystroglycan and heparin. *EMBO J.* **19**, 1432-1440.
- Xu, H., Wu, X. R., Wewer, U. M. and Engvall, E. (1994). Murine muscular dystrophy caused by a mutation in the laminin alpha 2 (Lama2) gene. *Nat. Genet.* **8**, 297-302.
- Yamada, H., Chiba, A., Endo, T., Kobata, A., Anderson, L. V., Hori, H., Fukuta-Ohi, H., Kanazawa, I., Campbell, K. P., Shimizu, T. and Matsumura, K. (1996). Characterization of dystroglycan-laminin interaction in peripheral nerve. *J. Neurochem.* **66**, 1518-1524.
- Yurchenco, P. D. (1994). Assembly of laminin and type IV collagen into basement membrane networks. In *Extracellular Matrix Assembly and Structure* (ed. P. D. Yurchenco, D. E. Birk and R. P. Mecham), pp. 351-388. New York: Academic Press.
- Yurchenco, P. D. and Cheng, Y. S. (1993). Self-assembly and calcium-binding sites in laminin. A three-arm interaction model. *J. Biol. Chem.* **268**, 17286-17299.
- Yurchenco, P. D. and Furthmayr, H. (1984). Self-assembly of basement membrane collagen. *Biochemistry* **23**, 1839-1850.
- Yurchenco, P. D. and O'Rear, J. J. (1994). Basement membrane assembly. In *Methods in Enzymology*, Vol. 245 (ed. E. Ruoslahti and E. Engvall), pp. 489-518. New York: Academic Press.
- Yurchenco, P. D., Cheng, Y. S. and Colognato, H. (1992). Laminin forms an independent network in basement membranes. *J. Cell Biol.* **117**, 1119-1133.
- Yurchenco, P. D., Sung, U., Ward, M. D., Yamada, Y. and O'Rear, J. J. (1993). Recombinant laminin G domain mediates myoblast adhesion and heparin binding. *J. Biol. Chem.* **268**, 8356-8365.
- Yurchenco, P. D., Quan, Y., Colognato, H., Mathus, T., Harrison, D., Yamada, Y. and O'Rear, J. J. (1997). The alpha chain of laminin-1 is independently secreted and drives secretion of its beta- and gamma-chain partners. *Proc. Natl. Acad. Sci. USA* **94**, 10189-10194.
- Zhong, C., Chrzanowska-Wodnicka, M., Brown, J., Shaub, A., Belkin, A. M. and Burridge, K. (1998). Rho-mediated contractility exposes a cryptic site in fibronectin and induces fibronectin matrix assembly. *J. Cell Biol.* **141**, 539-551.